N 70 28623
NASA CR 110150

THE PERKIN-ELMER CORPORATION
AEROSPACE SYSTEMS
2855 Metropolitan Place Pomona, California

DESIGN AND CONSTRUCTION OF HEATED ION SOURCE FOR ORGANIC ANALYSIS AND DESIGN AND CONSTRUCTION OF DOUBLE FOCUSING MASS SPECTROMETER ANALYZER

FINAL REPORT

December 1969

JPL Contract Number 952424
Perkin-Elmer Aerospace Systems SPO 30000

This work was performed for the Jet Propulsion Laboratory, California Institute of Technology, sponsored by the National Aeronautics and Space Administration under Contract NAS7-100.

Prepared for
CALIFORNIA INSTITUTE OF TECHNOLOGY
Jet Propulsion Laboratory
Pasadena, California

1 of 20

TABLE OF CONTENTS

LIST OF ILLUSTRATIONS

1. INTRODUCTION

The primary goal of the Viking Program is to determine the existence of life on Mars. The Pyrolysis-Gas Chromatograph-Mass Spectrometry (GC/MS) experiment offers an indirect approach to the question of life existence on Mars. The GC/MS identification does not depend on living organisms being present in a specific soil sample, but depends on a chemical interpretation of mass spectra of specific organic materials as indirect evidence of the existence or previous exisence of life. The instrumentation can also serve a dual purpose, for example, when the instrumentation is used without the pyrolysis-gas chromatograph sections it can also provide an analysis of the Martian atmosphere.

This report is concerned with the development of the mass spectrometer for a proposed GC/MS life detection system. The mass spectrometer which has been selected for this application is a double focusing sector instrument of the Johnson-Nier type. The mass spectrometer system must be constructed with strict regard for weight and size limitations and still obtain the required performance. The performance goals for the mass spectrometer systems are:

a. Ion source sensitivity: 1×10^{-6} A/torr

b. Ion source linearity: linear response of current versus pressure to a maximum pressure of 1×10^{-4} torr over the design mass range

c. Heated ion source temperature: $-250^{\circ}C$

A 90° electrostatic sector, 60° magnetic sector mass spectrometer was previously built by Perkin-Elmer on JPL Contract 952009. This instrument was primarily intended for atmospheric analysis. This final report covers the effort of JPL Contract 952424 and concerns the modification of the previous instrument in order to improve its performance, reduce its size, and make it more suitable for organic analysis. The primary modifications performed were:

a. The addition of an ion source heater for heating the ion source to $250^{\circ}C$.

b. The modification of the ion source magnet for increased field strength and placement of the anode outside of the ionizing region.

c. Change in analyzer geometry

d. Electric sector redesign.

The heated ion source is a needed addition because the capability of monitoring organics is required. Organics, in general, have a low vapor pressure and adhere readily to cold surfaces. Organics adhering to the surfaces of the ion source can cause charge up and cause instability which is not desired. Heating the ion source to 250°C will prevent this problem by reducing the adsorption of organics on the ion source surfaces.

In the previous ion source design, confinement of the electron was not obtained due to the weak magnetic field. In order to avoid excessive walking of the electron beam, it was necessary to operate with zero electrostatic gradient across the ionizing region. This is not compatible with linear operation to 1×10^{-4} torr. A new, more effective magnet design was required to eliminate this difficulty. The ion source was modified and the anode was placed outside of the ionizing region to maintain it at a lower pressure. The object of this change was to reduce the buildup of surface contamination on the anode and thereby improve the stability of the source.

The Mass Spectrometer System configuration was changed from the standard Nier geometry (90° electric sector -60° magnetic sector) to a 90° electric sector -90° magnetic sector system. The 90°-90° geometry has several advantages over the 90°-60° geometry. The primary advantage is that the instrument becomes smaller because the total ion path length is reduced and the additional bend in the analyzer reduces the distance between the ion source and the collector. Another advantage of the 90°-90° system is the structure is inherently more rugged because it is more compact. The new geometry does have one disadvantage in that a larger analyzer magnet is needed. However, the size and structural advantage outweighs the disadvantage of the increase in analyzer magnet weight.

The radius of the electric sector was changed to 1.86 inches and a different method of mounting the plates was used. The two outer plates were match bored to the rails with ruby pins as shown in Figure 1-1. The previous design is shown in Figure 1-2. The modifications made lead to a more compact and rugged design.

A limited amount of testing of the ion source was performed. Some problems were encountered but lack of funds prevented a complete solution. The results of the tests are also presented in this report.

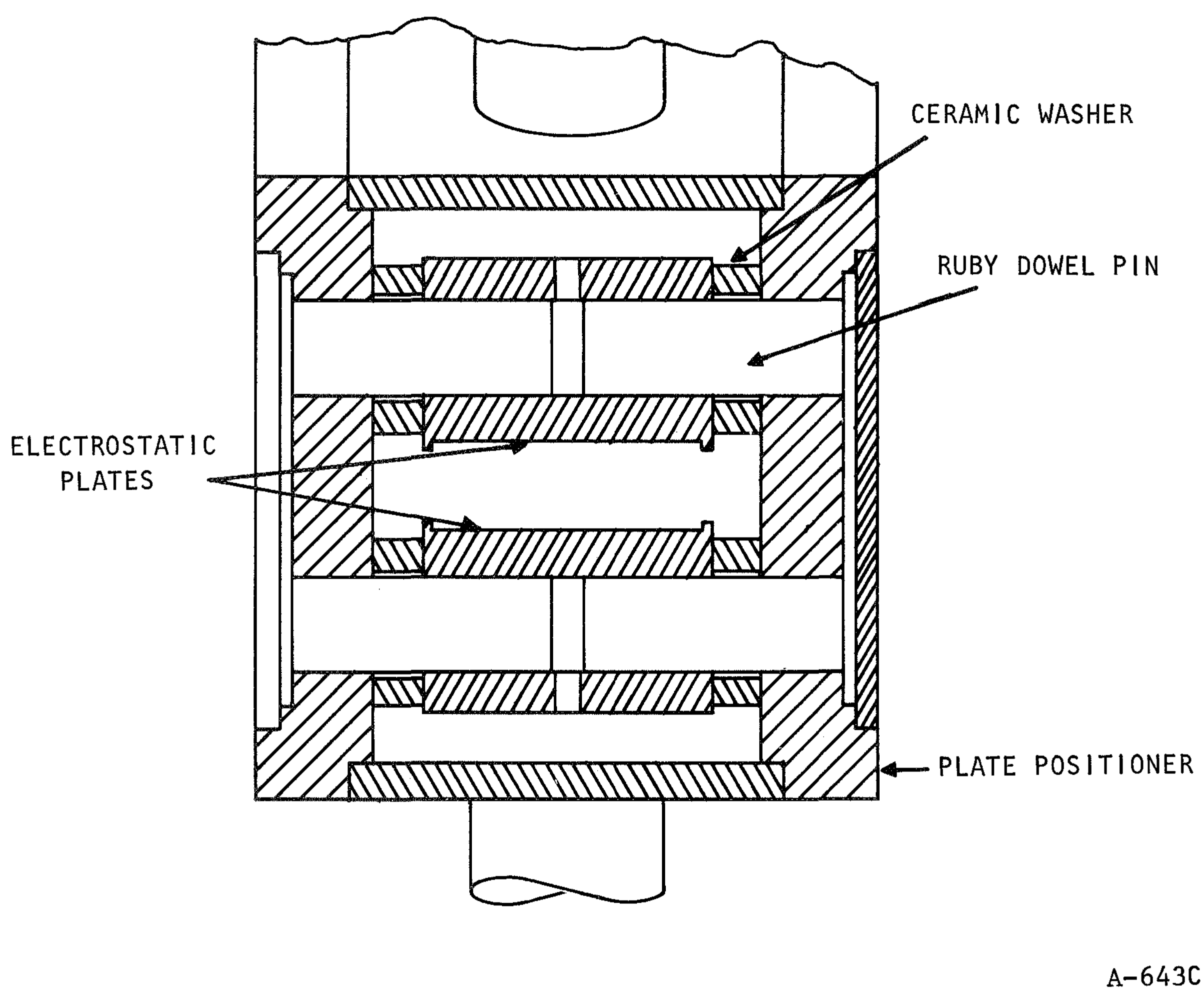

FIGURE 1-1. New Electric Sector Mounting Configuration

5

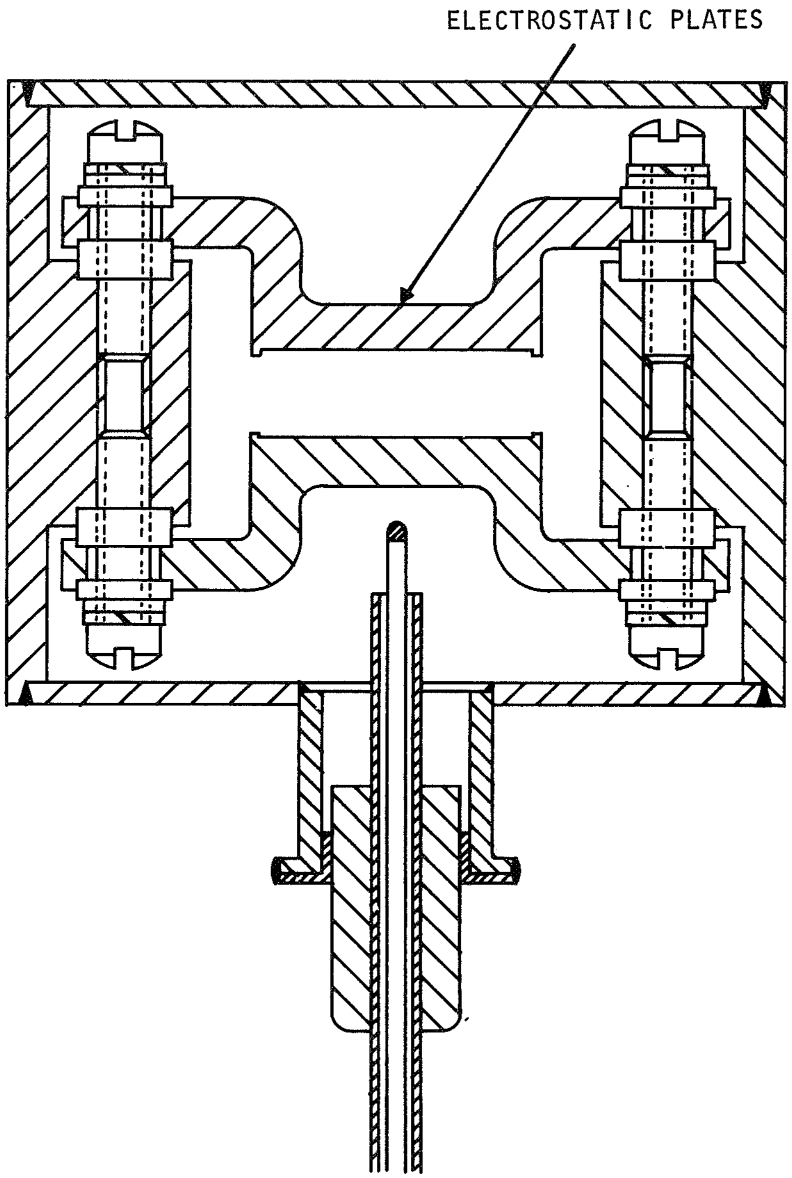

FIGURE 1-2. Old Method of Mounting Electric Sector

2. ION SOURCE MAGNET

The ion source design utilizes a hollow cylindrical magnet to collimate the electron beam. Electrons enter through one end, travel the length of the cylindrical magnet and are collected at the anode. The previous ion source magnet design utilized a double yoke magnet to collimate the electrons. Difficulty was encountered in obtaining a high enough field to provide effective collimation. Analysis showed that the gap flux density was only 30 gauss. The large leakage of this design and the lack of available space for additional magnet material yielded this low field strength and consequent walking of the electron beam in the E x B field. The bar magnets used on the previous ion source had to be placed outside of the diameter of the circular repeller which was used so that ion source sealing could be obtained by using circular ceramic sections. The distance between the bar magnets was so large that the magnetic field at the center of the chamber was due to excessive leakage. A new cylindrical magnet design was decided upon as a solution to the collimation problems. A drawing of the ion source magnet is shown in Figure 2-1.

The tubular source magnet is made of a permanent magnet material that is known as Cunife. Cunife, a copper, nickel, ion alloy, was chosen as the magnetic material because of its clean properties in a vacuum and its machinability. The magnet has magnetic field intensity at the knee of the BH curve, which is about 375 oersteds. This value of the field intensity matches the air gap field, since both the magnet and the air gap will have the same length. The magnet forms the walls of the ionization chamber and the ion accelerator. A repeller plate is extended into the tubular magnet from the anode end.

The curvature of the ion accelerator produces an ion ray divergence that is partially compensated for by the curvature of the repeller surface. Further convergence is obtained by the saddle lens.

Two slots are machined in the magnet. One slot is for the gas that is admitted into the ion source. The other slot provides an exit path for the newly formed ions. The addition of the slots detracts from the uniformity and magnitude of the field. A field of about 150 gauss was obtained in the center of the magnet. This is sufficient to collimate the electrons but some movement of the beam off the axis occurred because of the slots in the magnet.

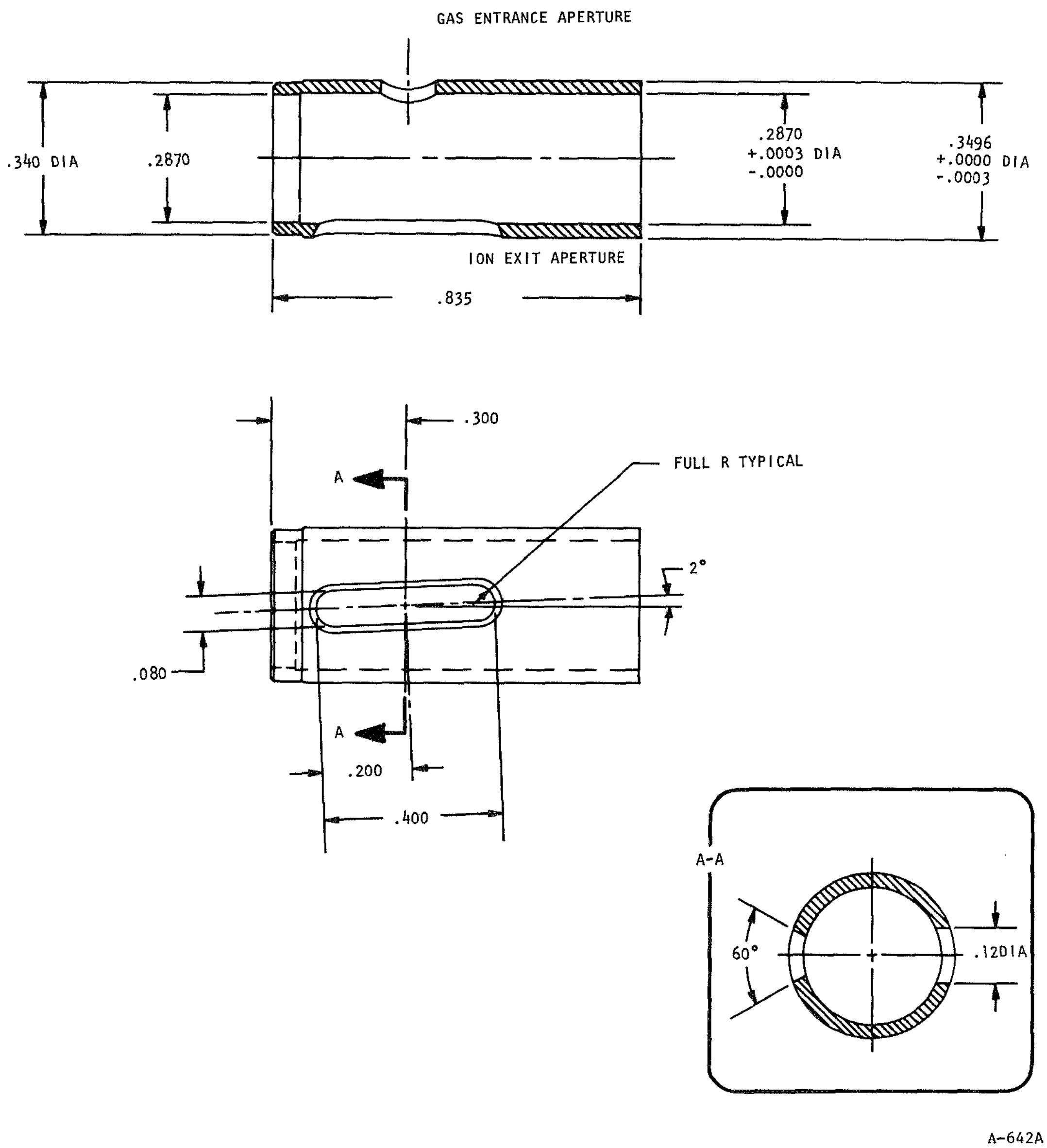

FIGURE 2-1. Ion Source Magnet

3. HEATERS

The ionization chamber of the ion source is designed to withstand a temperature of 250 ±5^{o}C. The Task I ion source has three heaters. One heater was mounted on each of the following existing ceramic pieces: the lens ceramic ring; the repeller ceramic ring; and the inlet ceramic tube. For the Task II ion source, beryllia ceramics were used to provide the heater supports and the electrical isolation necessary tc good thermal conductive paths. The thermal conductivity of beryllia is about a factor of ten times that of alumina.

The heater material is deposited on the ceramic support so that a good thermal contact is established. Vacuum evaporation is used to deposit the heater film. The heater film was made of chromium because it has a coefficient of thermal expansion that will allow a match with the ceramics.

Heat transfer calculations were made for the Task I ion source which gives the expected heater power that would be required to elevate the ionization chamber walls to a temperature of 250^{o}C. The expected power requirements are as listed:

	Minimum	Maximum
Inlet Tube	2.3 W	3.3 W
Repeller Ring	6.0 W	8.5 W
Lens Ring	12.9 W	18.2 W
TOTAL	21.2 W	30.0 W

The maximum power for a ring is expected to be 20 watts. For a 28 volt power supply, the required heater resistance is 40 ohms.

Laboratory experiments have shown that the source can be heated to 250^{o}C using 14 watts.

4. SOURCE MODIFICATION ANALYSIS

A primary objective of this contract was to modify the ion source, which was designed for JPL on a previous contract, so that the source would provide a linear response at a maximum source pressure of 10^{-4} torr, over the mass range of of 10 to 140 AMU. The sensitivity of the source should be at least 1×10^{-6} amperes per torr, over the complete mass range measured at the analyzer collector. The object slit is to have a width of 0.002 inch.

The design approach used on this contract was to utilize the previous ion source design and to make small modifications that would produce a performance improvement.

The following parameters were obtained from the previous source design:

l_{ar} = distance between the ion repeller and the ion accelerator

= 0.16 in

W = width of the electron beam

= 0.050 in

i = electron current in the ionization chamber

= 60 μA

The following definitions are useful for the analysis of the effects of space charge:

a = ratio of the distance between the electron beam and the ion accelerator to the distance between the ion repeller to the ion accelerator

$= l_{ab}/l_{ar}$

α = ratio of the electrical potential between the electrom beam and the ion accelerator to the electrical potential between the ion repeller and the ion accelerator

$= V_{ab}/V_{ar}$

i_v = ratio of the electron current to the repeller voltage

$= i/V_{ar}$

i_{vo} = the value of i_v that depresses the potential of the ionization plane to the potential of the ion accelerator at a zero source pressure

P_c = critical pressure

X = ratio of the source pressure to the critical pressure

$= P_s/P_c$

If $i_v/i_{vo} << 1$ the potential depression can be represented by the following linear equation

$$\propto \; = a[1 + (X - 1)i_v/i_{vo}]$$

Let $\propto_o = a(1 - i_v/i_{vo})$

$\simeq a$

$$\frac{\Delta\propto}{\propto} = Xi_v/i_{vo}$$

The demagnification factor of the exit aperture is given by:

$$G = \frac{\ell ab}{f_1}$$

f_1 = focal length

$$\frac{\propto V_{ar}}{E_1}$$

Where E_1 = electrical field intensity on the exit side of the slit

$$\frac{\Delta G}{G_o} \qquad \frac{\Delta\propto}{\propto_o}$$

If the image of the ion beam at the object plane is large, then at the exit slit, the variation in the transmitted ion beam would be equal to the variation in demagnification factor. A one percent change in the potential of the ionization plane would result in a one percent change in the transmitted ion current.

$$\frac{\Delta\propto}{\propto} \leq 0.01$$

The critical pressure is given by

$$P_c = 3(V_{ar} m_e / aV_{e\ell} m_i)^{1/2} \quad 4S\ell_{ar}$$

Where m_e = mass of the electron

m_i = mass of the ion

S = ionization probability

$V_{e\ell}$ = acceleration potential of the electrons

= 70 volts

$$P_c = 1.6 \times 10^{-3} \sqrt{\frac{V_{ar}}{aM}} \text{ torr}$$

$$X = \frac{10^{-4}}{P_c} = 6.25 \sqrt{\frac{aM}{V_{ar}}} \times 10^{-2}$$

$$X\, i_v / i_{vo} < 0.01$$

$$6.25 \sqrt{\frac{aM}{V_{aM}}} \times 10^{-2} \times \frac{60}{V_{aM} i_{vo}} \leq 0.01$$

$$i_{vo} = \frac{\Sigma_o W 10^6}{\ell_{ar}(1-a) \frac{m_e}{2V_{e\ell} e}}$$

Where e = electronic charge

Σ_o = permittivity of free space

$i_{vo} = \frac{14}{1-a}$ microamperes/volt

The required repeller voltage is given by

$$V_{aM} = [26.8\ (1-a) \sqrt{aM}]^{2/3}$$

Let $a = 0.9$

$M = 140$

$V_{ar} = 21.6$ volts

The electron beam is deflected to one side because of the combined forces of the repeller field and the magnetic field. The deflection angle, Ω, is given by:

$$\tan\Omega = \frac{V_{aM}}{\ell_{aM} B_s \sqrt{2V_e \ell\ e/me}}$$

$$= 0.035$$

$$\Omega = 2^{o}$$

The slits in the ion focal system are rotated two degrees so that they are aligned with the electron beam. The electron entrance aperture is offset so that the slits can be centered. The electron entrance aperture is given by:

$$Y_{o.s.} = \frac{\ell_r M}{2} = \tan\Omega$$

Where ℓ_r = length of the repeller

= 0.46 inch

$Y_{o.s.} = 0.08$ inch

The mass discrimination that occurs in the source is characterized by a deflection in the Y direction that is given by:

$$Y_1 = \frac{1}{3} \ell_{ab}{}^2 B_s \sqrt{\frac{2q}{V_{ab}\ m_i}}$$

Where Y_1 = deflection at the ion accelerator

ℓ_{ab} = distance between the ion accelerator and the ion beam

q = ionic charge

The deflection of one mass can be compensated for by the electrostatic deflection of the split lens; however, the difference in the deflection for ions that have masses which are located at the extremes of the mass range cannot be compensated for. This difference is given by:

$$\Delta Y = \frac{1}{3} \ell_{ab}{}^{2} B_s \sqrt{\frac{2q}{V_{ab}}} \left[\frac{1}{m_{i,1}} - \frac{1}{m_{i,2}} \right]$$

$$= 3.9 \text{ inch}$$

If the image size is less than the object slit size, the sensitivity would be greatly reduced on one end of the mass scan range because of the source mass discrimination. The variation in sensitivity would be less severe if the image size is greater than object slit size, but the overall sensitivity would be reduced.

The repeller voltage cannot be scanned with the ion acceleration voltage because of the electron beam deflection. With such a large fixed voltage, a uniform ion focus over the mass scan range would be impossible. For this reason, a saddle lens is used to reduce the velocity of the ions after they leave the ionization chamber and the magnetic field. This lens will reduce the energy of the ions to approximately four electron volts as they enter the ion focusing system.

5. ANALYZER GEOMETRY

The previous JPL instrument had a 90^{o} electric sector and a 60^{o} magnetic sector. This configuration was modified to a 90^{o} electric sector -90^{o} magnetic sector utilizing the following nominal dimensions:

Magnetic Sector Radius	R_m	= 1.50 in
Electric Sector Radius	R_e	= 1.86 in
Electric Sector Object and Image Distance	$1_e^{1} = 1_e^{11}$	= 0.652 in
Magnetic Sector Object Distance	1_m^{1}	= 2.217 in
Magnetic Sector Image	1_m^{11}	= 1.018 in
Magnetic Sector Angle	ϕ_m	= 90^{o}
Electric Sector Angle	ϕ_e	= 90^{o}

The 90^{o}-90^{o} configuration has the advantages over the 90^{o}-60^{o} configuration in that the object distance becomes shorter. A disadvantage occurs in that a larger magnet is used. A layout of the instrument is shown in Figure 5-1.

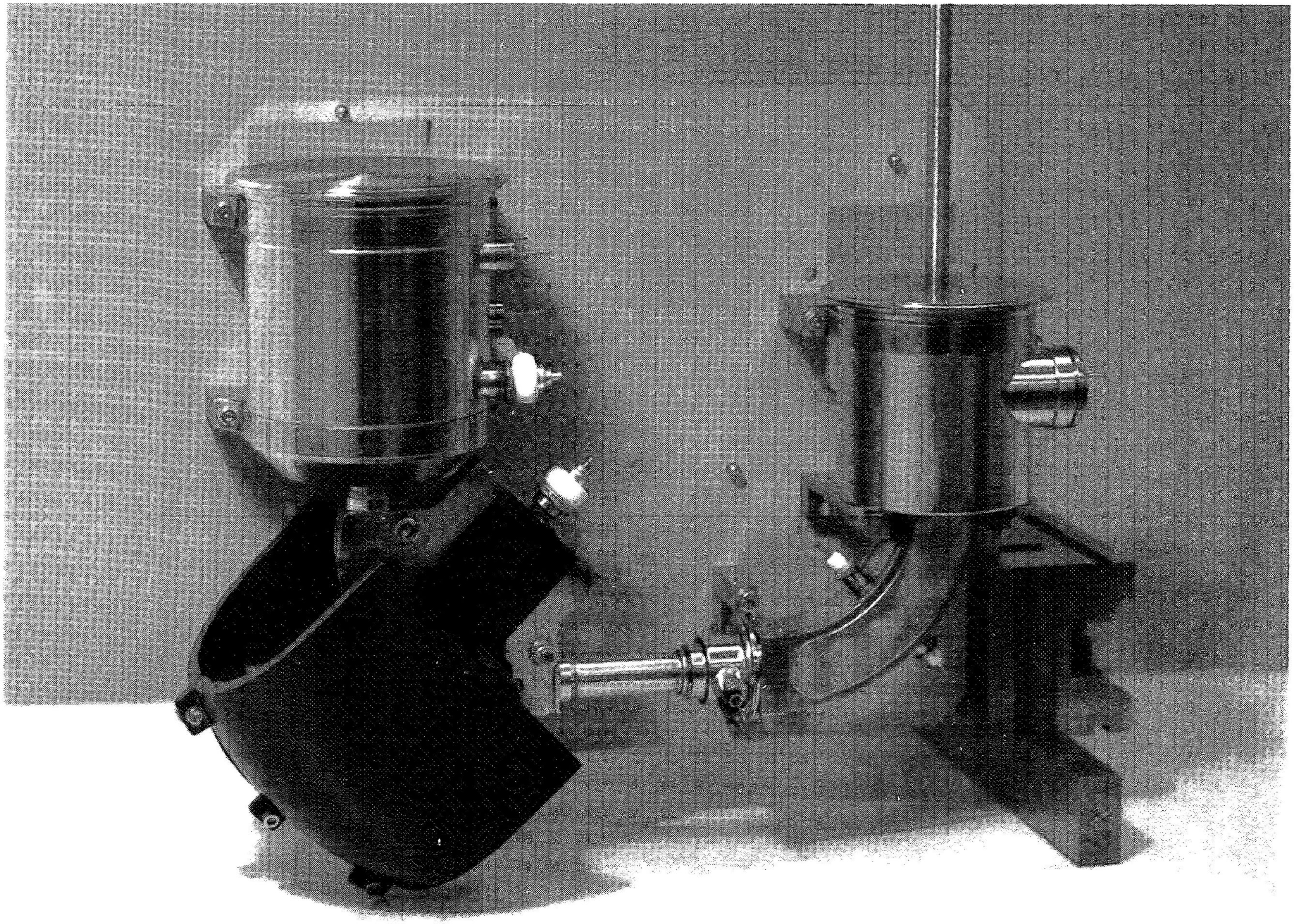

FIGURE 5-1. 90°-90° Electric and Magnetic Sector Layout

6. ION SOURCE TESTING

The ion source design utilized a new method of collimating the electrons. A cylindrical magnet of cunife collimates the electrons and also provides the chamber in which the ions are formed. The cylinder has two openings on two sides. The gas molecule enters through one hole and the ions exit through the other hole. The primary problem encountered in testing was that the electrons would drift to one side and collect on the ion chamber.

The ion source cylindrical magnet is shown in Figure 2-1. The axial magnetic field was plotted and is shown in Figure 6-1. During the initial test phases difficulty occurred in aligning the filament in the correct position above the electron entrance aperture. Initial tests show that the spot burnt on the electron entrance aperture plate was not aligned over the aperture because the filament was bent.

The electron gun electrodes were fabricated of magnetic stainless steel so that the electron beam would be shielded from the magnetic field while it was in the electron gun. This would, in theory, allow the electron beam to be focused by electrostatic fields thereby leading to a more intense beam.

In all cases less than 25 percent of the electron beam entered the ionization chamber. The poor transmission of the electron beam and the bending of the filament indicated that there was sufficient magnetic field in the electron gun region to cause undesirable effects upon the electron beam focusing as well as deflection of the filament. Little time was used in trying to correct this problem. It was decided that worthwhile tests could be run even with the filament not aligned. Testing was continued to determine if transmission of the electron beam occurred through the interior of the bar magnet to the anode. The electron entrance aperture was offset 0.008 inch from the exit aperture to the anode in order to allow for some deflection of the beam in the E x B field. The electron entrance aperture had a cross sectional dimension of 0.010 x 0.0 while the aperture allowing exit to the anode had dimensions of 0.014 x 0.093 inch. The lengths of these two apertures were adjusted so that in combination with the ion exit aperture they would have a total conductance of 50 cc/sec for nitrogen. Initial tests of the transmission through these apertures showed that essentially more of the electron beam current was reaching the anode. Adjustment of the repeller-accelerator field provided no improvement. The uniformity of the magnetic field was immediately suspected.

Tests were run with repeller and anode adapter removed. This test determined where the electron beam was going as a result of the magnetic field only. A target was added on which the electron beam could burn a spot. The electron

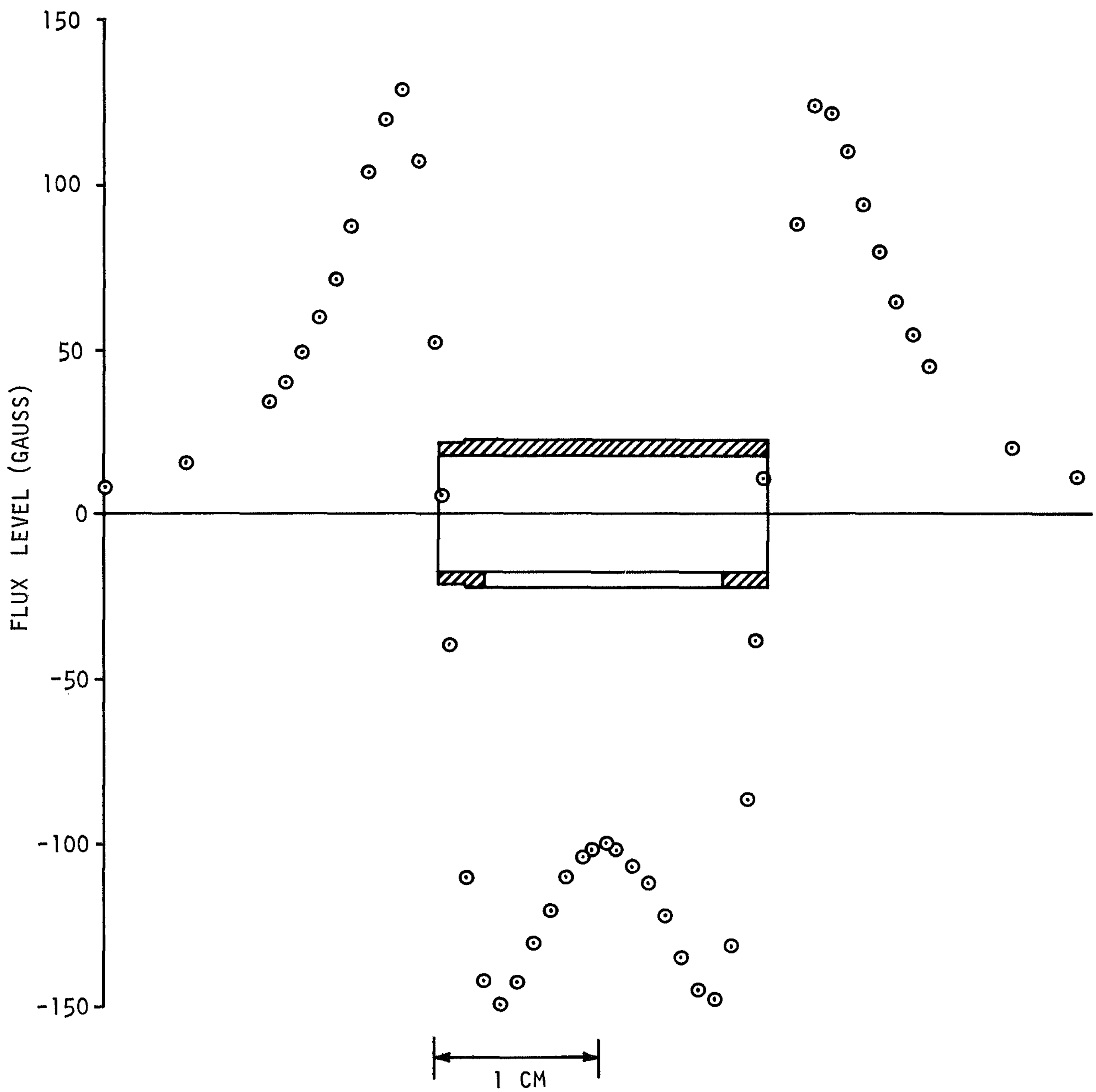

A-645C

FIGURE 6-1. ION SOURCE MAGNET FIELD PLOT beam made a spot on the target plate in the lower right hand corner position of the opening to the anode indicating that some distortion existed in the magnetic field.

Next the source magnet was removed and replaced by the cylindrical magnet without the gas entrance hole or ion exit slit. The new pattern received was good. The spot was in the center at the anode slit opening.

This result indicated that the slots in the magnet were causing the problem. The field lines inside the slotted cylinder were not straight but curved in the middle of the magnet. These curved field lines allowed the electrons to hit one side of the repeller and not be collected. This was confirmed by direct measurement of the magnetic field with a gauss meter.

Several modifications were tried in an attempt to improve the electron beam transmission to the anode. First, the gas entrance was modified so that the hole in the repeller side of the magnet could be eliminated and thereby improve the uniformity of the field along the paths of the electron beam. However, this was not confirmed during transmission tests. Next, a magnet with equal sized slots for the gas entrance and ion exit was tried in an attempt to obtain a more uniform and symmetrical field distribution. Again, the results were negative, the electron beam was found to hit the outer edge of the anode target. Several tests were run charging the magnet to determine if this had a significant effect upon field uniformity. Using a charging coil could possibly be causing nonuniformity and, therefore, a technique was tried in which a larger permanent magnet was used to charge the small ion source magnet with a noticeable improvement.

Attention was then directed to another area. The anode was made of magnetic material and effectively formed one of the pole pieces of the magnet assembly. Since the anode had to be electrically isolated from the magnet, a ceramic spacer was employed. This prevented good magnetic coupling between the anode and the magnet. Test results indicated that the electron beam was being deflected as it approached the anode and that field distortion was created by the improper coupling of the anode and bar magnet. The alumina ceramic spacer was replaced by one of barium ferrite. This material gave the necessary electrostatic insulation while having a high permeability for good magnetic coupling. In spite of the expected improvement, none was observed.

Another source of difficulty was discovered while reassembling the ion source. The repeller electrode was found to exhibit some residual magnetism which was probably a contributing factor to the inadequate collimation of the electron beam. Not only was this a possible source of degradation, but it also indicated that the part had a permeability greater than that of air. This would lead to a redistribution of the magnetic field when the repeller was placed inside of the magnet. The repeller and other supposedly nonmagnetic electrodes were fabricated of 304 stainless steel which can become magnetized to a significant degree by cold working. Evidently, during the machining of the part it had been cold worked sufficiently to cause the magnetic properties. The magnetic pieces were sent out for heat treating but further testing was precluded due to funding limitations. Investigation of the cold working problem showed that 316 stainless steel and Carpenter No. 10 maintain their nonmagnetic properties much better than 304 stainless steel and, therefore, these materials are recommended for further applications when nonmagnetic materials are required.

7. CONCLUSIONS

The effort carried on under JPL Contract 952424 led to the development of a prototype mass spectrometer for application in the soil analysis experiment on the Viking Lander. Difficulties encountered during the experimental phase of the effort precluded the verification of specific performance parameters. A limitation in the funding prevented the completion of the necessary design modifications which would have led to a successful instrument. The difficulty of designing a uniform magnetic field in a region with a closely spaced magnetic field in a region with a closely spaced magnetic circuit of comparagle dimensions was the primary cause of the delay in achieving full test results. Continued modification and testing at JPL has led to the successful resolution of the problems which have been discussed.